# Correlation between microarray DNA hybridization efficiency and the position of short capture probe on the target nucleic acid

Régis Peytavi, Liu-ying Tang, Frédéric R. Raymond, Karel Boissinot, Luc Bissonnette, Maurice Boissinot, François J. Picard, Ann Huletsky, Marc Ouellette, and Michel G. Bergeron

*BioTechniques 39:89-96 (July 2005)*

*The hybridization behavior of small oligonucleotides arrayed on glass slides is currently unpredictable. In order to examine the hybridization efficiency of capture probes along target nucleic acid, 20-mer oligonucleotide probes were designed to hybridize at different distances from the 5′ end of two overlapping 402- and 432-bp* ermB *products amplified from the target DNA. These probes were immobilized via their 5′ end onto glass slides and hybridized with the two labeled products. Evaluation of the hybridization signal for each probe revealed an inverse correlation with the length of the 5′ overhanging end of the captured strand and the hybridization signal intensity. Further experiments demonstrated that this phenomenon is dependent on the reassociation kinetics of the free overhanging tail of the captured DNA strand with its complementary strand. This study delineates key predictable parameters that govern the hybridization efficiency of short capture probes arrayed on glass slides. This should be most useful for designing arrays for detection of PCR products and nucleotide polymorphisms.*

## INTRODUCTION

Over the last decade, DNA microarrays have become useful tools in genomic studies and drug discovery (1–3). Unlike other hybridization formats, microarrays allow significant miniaturization, as thousands of different DNA fragments or oligonucleotide probes can be spotted onto a solid support, generally a glass slide. Therefore, this technology is ideal for extensive gene profiling studies and multiplexed detection of nucleic acids for diagnostic purposes. While microarrays have been widely used in gene expression profiling, there is great potential for the detection and identification of single-nucleotide polymorphisms (SNPs) and for the diagnosis of disease. Examples of useful applications include cancer prognostics (4–6), forensic science (7), detection of microbes and their associated resistance genotypes (8,9), and detection of bioweapon pathogens (10).

While DNA probes longer than 70 nucleotides give reproducible hybridization signals (11,12), only short oligonucleotides (15–20 bases long) allow efficient discrimination of SNPs (13,14). However, the hybridization efficiency of short probes is still unpredictable, and false-negative results are often observed when short surface-bound DNA probes are used on microarrays. Many parameters are suspected to influence the hybridization efficiency of target DNA to immobilized oligonucleotide DNA probes. These parameters include steric hindrance, secondary structure of the target DNA, and binding capacity of the surface-bound probe. Steric hindrance may vary with probe density, spacer length, as well as hydrophobicity and charge of the solid support (15). Secondary structure of the target DNA was shown to influence the intensity of hybridization and could be relieved by using helper oligonucleotides hybridizing beside the probe (12,16). The influence of target secondary structure could be partially circumvented by selecting probes for their theoretical thermodynamic behavior (17). In addition, the use of single-stranded targets instead of denatured, double-stranded PCR products has been found to increase the sensitivity of the hybridization reaction on short probes meaning that the complementary strand may interfere with the hybridization of targets onto the capture probes (16,18,19). Moreover, the design of short oligonucleotide probes that are both sensitive and specific enough to discriminate SNPs is not easily predictable by capture probe melting temperature ($T_m$) (12,20). Thus, oligonucleotide design is done either empirically (21,22) or by software using heuristic algorithms (23).

Different research groups have noticed that hybridization efficiency is dependent on the position at which the probe binds on the target nucleic acid, although no explanations were provided for these observations (15,16). In one study, it was noted that hybridization was not optimal when using probes positioned close to one end of the PCR product, but it was concluded that this was mainly due to secondary structure issues (24). In another study (25), a strong binding preference for 59-bp probes sharing sequence identity with a 3′ region (targeting a 5′ end) of nondenaturated large products has been observed. It was demonstrated that multi-stranded DNA structures, including the target double-stranded labeled DNA, are preferentially formed

Centre Hospitalier Universitaire de Québec, Sainte-Foy, Québec, Canada

**Table 1. Oligonucleotide Primers and Probes Used in this Study**

| Primers | Sequence | Target Gene | Product Length (bp) |
|---|---|---|---|
| ErmB225 | 5′-TCGTGTCACTTTAATTCACCAAGATA-3′ | *ermB* | 402 |
| ErmB601 | 5′-TTTTTAGTAAACAGTTGACGATATTC-3′ | *ermB* | |
| ErmB109 | 5′-GGAACAGGTAAAGGGCATTTAACGAC-3′ | *ermB* | 432 |
| ErmB512 | 5′-CTGTGGTATGGCGGGTAAGTTTTATTAAG-3′ | *ermB* | |
| TShoH240 | 5′-GCTTTAGAAGGCGATGCTCAATACG-3′ | *tuf* | 523 |
| TStaG765 | 5′-TIACCATTTCAGTACCTTCTGGTAA-3′ | *tuf* | |
| shv604 | 5′-CAGCTGCTGCAGTGGATGGT-3′ | $bla_{SHV}$ | 182 |
| shv449 | 5′-AGATCGGCGACAACGTCACC-3′ | $bla_{SHV}$ | 337 |
| shv368 | 5′-TTACCATGAGCGATAACAGC-3′ | $bla_{SHV}$ | 418 |
| shv313 | 5′-AGCGAAAAACACCTTGCCGAC-3′ | $bla_{SHV}$ | 473 |
| shvseq71 | 5′-AGCCGCTTGAGCAAATTAAACTA-3′ | $bla_{SHV}$ | 715 |
| shv763 | 5′-GTATCCCGCAGATAAATCACCAC-3′ | $bla_{SHV}$ | reverse primer |
| **Probes** | | | |
| A-S-ErmBH272 | 5′-CAAACAGAGGTATAAAATTG-3′ | *ermB* | |
| A-S-ErmBH370 | 5′-TGATTGTTGAAGAAGGATTC-3′ | *ermB* | |
| A-S-ErmBH459 | 5′-TTGCTTAAGCTGCCAGCGGA-3′ | *ermB* | |
| A-S-ErmBH272a | 5′-CAATTTTATACCTCTGTTTG-3′ | *ermB* | |
| A-S-ErmBH370a | 5′-GAATCCTTCTTCAACAATCA-3′ | *ermB* | |
| A-S-ErmBH459a | 5′-TCCGCTGGCAGCTTAAGCAA-3′ | *ermB* | |
| A-S-TShoH713 | 5′-ATACGTTTTATCAAAAGATGAAG-3′ | *tuf* | |
| A-S-TStaGH554 | 5′-TACTGGTGTAGAAATGTTC-3′ | *tuf* | |
| A-S-TShoH520a | 5′-GAAGTTTCTTTGATACCAAT-3′ | *tuf* | |
| A-S-TShoH520 | 5′-ATTGGTATCAAAGAAACTTC-3′ | *tuf* | |
| A-S-Shv1H691 | 5′-CCCCGCTCGCCAGCTCCGGT-3′ | $bla_{SHV}$ | |

via single strand association with the homologous 5′ strand near the end of arrayed DNA probes.

In this work, we have attempted to understand the hybridization behavior of short oligonucleotides anchored by their 5′ end (26) onto a solid support, using as a model system the detection of several genes. We show that the efficiency of hybridization of 20-mer capture probes to PCR products is highly dependent on their positions on the product. We provide evidence that kinetic effects and reassociation to the PCR product's complementary strand can lead to destabilization of the capture probe/DNA target duplex and that this kinetic effect is governed by the position of the complementary sequence on targeted nucleic acids.

## MATERIALS AND METHODS

### Microarray Production

Twenty-mer oligonucleotide probes bearing a 5′ amino linker were synthesized by Biosearch Technologies (Novato, CA, USA). Probe sequences are listed in Table 1.

The amino linker modification allowed covalent attachment of probes onto aldehyde-coated glass slides (CEL Associates, Pearland, TX, USA). Oligonucleotide probes were diluted 2-fold in ArrayIt™ MicroSpotting Solution Plus (Telechem International, Sunnyvale, CA, USA) to a final concentration of 5 µM. Oligonucleotides were spotted in triplicate using a VIRTEK SDDC-2 arrayer (Bio-Rad Laboratories, Hercules, CA, USA) with SMP3 pins from Telechem International. After spotting, slides were dried overnight, washed by immersion in 0.2% sodium dodecyl sulfate (SDS; Laboratoire Mat, Québec, QC, Canada) for 2 min, and rinsed in ultrapure water for 2 min. Slides were boiled in ultrapure water for 5 min for washing out the unbound oligonucleotides. Imine bonds between the glass surface and probes were reduced to a stable amide link by immersion into a sodium borohydride solution (1 g sodium borohydride; Sigma, St. Louis, MO, USA), 300 mL phosphate-buffered saline (PBS; also from Sigma), and 100 mL ethanol for 20 min. Slides were then washed in 0.2% SDS for 1 min and rinsed in ultrapure water for 1 min. Slides were finally dried by centrifugation for 5 min under vacuum with a Savant SpeedVac™ Plus (Thermo Savant, Holbrook, NY, USA) and stored in a dry oxygen-free and dark environment. All above chemical treatments of the slides were performed at room temperature.

### PCR Amplification and Product Labeling

Fluorescent dyes were incorporated during PCR amplification. Cy™3 or

Cy5 dUTP (Amersham Biosciences, Baie d'Urfé, QC, Canada) were mixed at concentrations of 0.02 µM in a 50-µL PCR mixture containing 0.05 mM dATP, 0.05 mM dCTP, 0.05 mM dGTP, 0.02 mM dTTP, 5 mM KCl, 1 mM Tris-HCl (pH 9.0), 0.01% Triton® X-100, 2.5 mM $MgCl_2$, 0.5 U *Taq* DNA polymerase (Promega, Madison, WI, USA), 1 ng purified genomic DNA, and 0.2 µM of each of the two primers. To test the effect of oligonucleotide probe position on the captured target DNA strand on hybridization efficiency, we amplified two overlapping PCR portions (402 and 432 bp) of the *Staphylococcus aureus ermB* gene (Figure 1). The *ermB* gene was amplified from genomic DNA isolated from the erythromycin-resistant *S. aureus* strain CCRI-1277. The 402-bp product was produced using primers ErmB225 and ErmB601 (Table 1), while the 432-bp product was amplified by PCR using primers ErmB109 and ErmB512 (Table 1). The *tuf* gene was amplified from genomic DNA isolated from the *Staphylococcus hominis subsp. hominis* strain ATCC 27844. A 523-bp product was produced using primers TshoH240 and TstaG765 (Table 1). The $bla_{SHV}$ gene was amplified from DNA isolated from *Escherichia coli* strain CCRI-1192. Different products were generated by combining the reverse primer shv763 with five different primers used to produce different 5′ overhanging tails: (*i*) primer shv604 amplified a 182-bp product; (*ii*) primer shv449 amplified a 337-bp product; (*iii*) primer shv368 amplified a 418-bp product; (*iv*) primer shv313 amplified a 473-bp product; and (*v*) primer shvseq71 amplified a 715-bp product (Table 1).

Thermal cycling for PCR amplification (180 s at 94°C, followed by 40 cycles of 5 s at 95°C, 30 s at 55°C, and 30 s at 72°C) was carried out on an MJ Research PTC-200 DNA Engine® thermal cycler (Bio-Rad Laboratories). PCR products were purified using the QIAquick® PCR purification kit (Qiagen, Mississauga, ON, Canada). The dye incorporation was measured with an Ultrospec 2000 Spectrophotometer (Amersham Biosciences) at 550 nm for Cy3 and at 650 nm for Cy5. Concentration of the amplified product was determined at 260 nm using the Ultrospec 2000.

Asymmetric PCR was performed using the PCR conditions described above, except that the upper strand was obtained using 20:1 ratio of ErmB109 and ErmB512 primers, respectively. An asymmetrical PCR was performed to produce the lower strand using 20:1 ratio of ErmB512 and ErmB109, respectively (Figure 1). Each asymmetric PCR was verified on a 1.5% agarose gel to ensure the production of single-stranded DNA and quantified using the Ultrospec 2000 at 260 nm. The concentration of single-stranded DNA was adjusted to 1 pM and hybridized to the microarray to confirm the absence of the complementary strand.

## DNA Microarray Hybridization and Data Acquisition

Prehybridization and hybridization were performed in 15 × 13 mm HybriWell™ self-sticking hybridization chambers (GraceBio-Labs, Bend, OR, USA). Microarrays were first prehybridized for 30 min at room temperature with 1× hybridization solution (6× standard saline phosphate-EDTA [SSPE; EM Science, Gibbstown, NJ, USA], 1% bovine serum albumin [BSA], 0.01% polyvinylpyrrolidone [PVP], 0.01% SDS, and 25% formamide [all from Sigma]). Cy-dUTP-labeled PCR products were denatured at 95°C for 5 min and then quickly chilled on ice. Five microliters of denatured labeled products

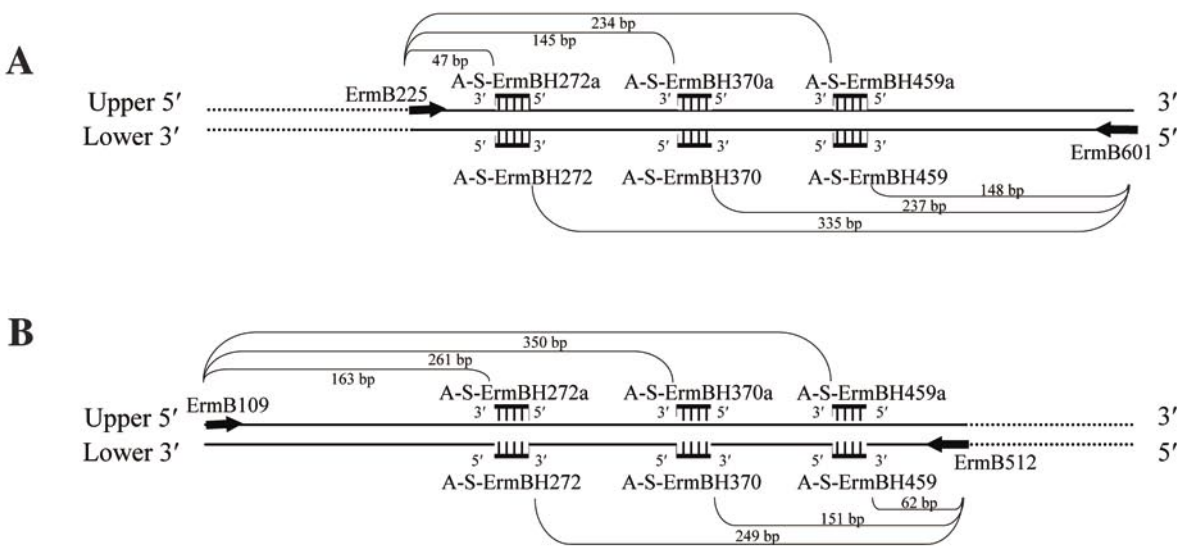


**Figure 1. Position of capture probes and PCR primers on the e*rmB* gene.** Arrows represent primers used for generating the products. Dashed boxes represent 5′ amino-modified probes. Brackets indicate the length of the 5′ overhanging tail for each capture probe. (A) The 402-bp *ermB* product. (B) The 432-bp *ermB* product.

were mixed with 10 µL of 2× hybridization buffer (12× SSPE, 2% BSA, 0.02% PVP, and 0.02% SDS) and 5 µL formamide (final concentration of 25%). Prehybridization solution was removed from the chamber and replaced by the labeled products resuspended in hybridization solution. The hybridization was carried out at 22°C for 15 min and up to 16 h. After hybridization, microarrays were washed with 2× SSPE containing 0.1% SDS for 5 min at room temperature and rinsed once with 2× SSPE for 5 min. Microarrays were dried by centrifugation at 1350× *g* for 3 min. Slides were scanned using a ScanArray® 4000XL confocal scanner (Packard Bioscience Biochip Technologies, Billerica, MA, USA), and fluorescent signals were analyzed using its software.

## RESULTS

In this work, we tested whether the region of the product targeted by an oligonucleotide capture probe influenced hybridization efficiency. To achieve this goal, we initially used the *ermB* bacterial antibiotic resistance gene as genetic target. This gene encodes an adenine N-6-methyltransferase, which confers resistance to macrolides, lincosamides, and streptogramin B (27). We generated two overlapping *ermB* products, each targeted by six 20-mer capture probes located at different areas of the products (Figure 1). Three of these probes (A-S-ErmBH272, A-S-ErmBH370, and A-S-ErmBH459) were designed to be complementary to the lower strand of both products, while the three other probes (A-S-ErmBH272a, A-S-ErmBH370a, and A-S-ErmBH459a) targeted the same region but hybridized to the upper strand of both products. For these perfectly complementary oligonucleotides, both strands have the same $T_m$ and secondary structure and have been shown to behave identically for hybridization in solution (28). Therefore, variations in the performance of hybridization between capture probes targeting the same region located on the opposite strand of a product could be attributed to a bias correlated with hybridization onto solid support.

The Cy3-labeled 402- and 432-bp products were hybridized overnight to the *ermB* array that contained the six different capture probes (Figure 1). After washing and analysis, it was observed that the fluorescence signal for each capture probe after overnight hybridization was not identical. Plotting the fluorescence intensities of hybridization against the regions of the product recognized by capture probes revealed a correlation between the fluorescence intensity and the length of the free 5′ overhanging portion of the captured strand (Figure 2). For each of the six capture probes, the strongest hybridization signal was always observed for the probe targeting a region closest to the 5′ end of the upper or lower targeted strand. These probes hybridized the closest to the 5′ end of the complementary strand of the product, thus leaving the shortest overhanging 5′ end. Both target products (402- and 432-bp) behaved similarly with respect to fluorescence intensity and position of the capture probe. Also, no difference was observed between the upper and lower strands. This is illustrated in Figure 2B

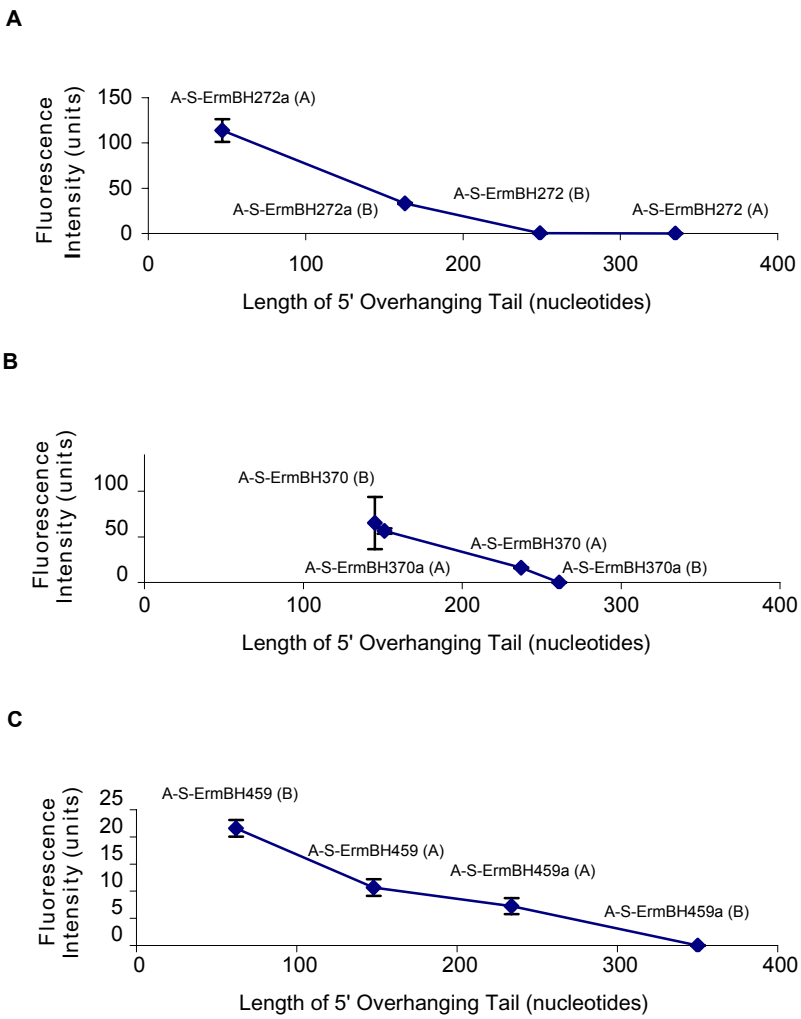


**Figure 2. Correlation between the fluorescence intensity and the length of the 5′ overhang of the captured *ermB* product strand.** (A) Results for probes A-S-ErmBH272 and A-S-ErmBH272a hybridized to the 402- and 432-bp *ermB* products. (B) Hybridization of probes A-S-ErmBH370 and A-S-ErmBH370a to the 402- and 432-bp *ermB* products. (C) Hybridization of probes A-S-ErmBH459 and A-S-ErmBH459a to the same two products. For all panels, each value represents the mean of three replicates. Standard deviation for these replicates is also shown.

by hybridization with oligonucleotides ErmB370 of product B, 151 bp from the 5′ end, and ErmB370a of product A, 145 bp from the 5′ end, showing that when the 5′ overhang lengths were similar, the fluorescence intensities were also similar regardless of the product size or the target strand.

To demonstrate that these rules are applicable to other DNA targets, we have tested the hybridization efficiency of different capture probes (according to the region to which they hybridize) on the highly conserved *tuf* gene, which encodes for elongation factor Tu (29), and on the $bla_{SHV}$ resistance gene, which encodes a β-lactamase (30). Results were similar to those obtained with *ermB*. Capture probes gave stronger hybridization signal when the 5′ overhanging tail was short and showed near background signals when the 5′ tail reached a length over 600 nucleotides for $bla_{SHV}$ and 250 nucleotides for *tuf* (Figure 3). Thus, different capture probes seem to follow similar hybridization rules, irrespective of the target sequences.

Results obtained with the $bla_{SHV}$ gene are particularly interesting. Products were produced using the same reverse primer but using different forward primers. This allowed the amplification of products having a variable forward length, while its reverse length remained constant. After hybridization of each product to the microarray, we plotted the signal in function of the length of the 5′ tail for the probes targeting the upper strand and in function of the length of the 3′ tail for the probes targeting the lower strand. The increase of the length of the 5′ tail reduced the signal (correlation coefficient between -0.66 and -0.85), whereas the increase of the 3′ tail had no major effect on the hybridization signal (correlation coefficient between 0.12 and 0.20). Those results suggest that, while the length of the 5′ tail has a significant impact on the hybridization signal observed, the length of the 3′ tail seems not important (data not shown).

Despite the fact that for the same oligonucleotide capture probe the key determinant for hybridization intensity appears to be the length of the 5′ overhang of the hybridized target DNA strand, some probes worked better than others. For example, in our system, probe A-S-ErmBH272a (5′ overhang length of 47 bp) produced a hybridization signal six times stronger than probe A-S-ErmBH459 (5′ overhang length of 62 bp). One explanation could be that the area covered by probe A-S-ErmBH459 may be less available for hybridization or less stable once hybridized than the area covered by probes A-S-ErmBH272-272a (Figure 2). This behavior could be attributed either to the secondary structure of the target strand or to thermodynamic properties of the probes. It is salient to point out that the ΔG of the secondary structure from probe A-S-ErmBH459 is -14.2 kcal/mol, which represents a much higher energy than that for the other probes used in this study (-5.3 kcal/mol for probe A-S-ErmBH272 and -3.5 kcal/mol for probe A-S-ErmBH370). Nonetheless, even if probe A-S-ErmBH459 gave a lower hybridization signal, its intensity correlated with the length of the 5′ tail (Figure 2 C).

Thus, capture probes (P) targeting the 5′ end of the captured target strand (T*) gave strong and repro-

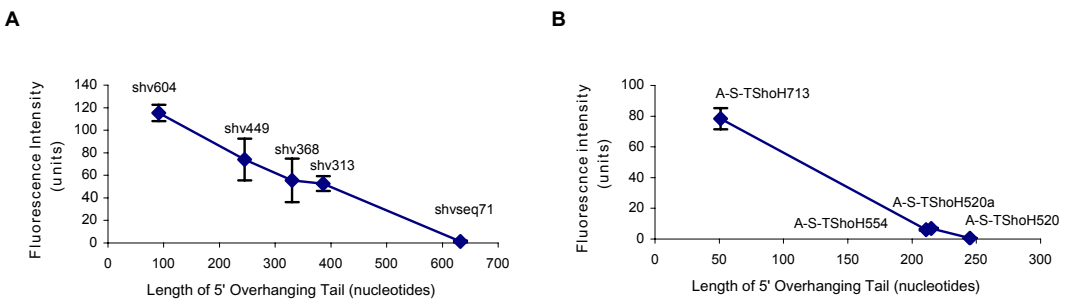


**Figure 3. Correlation between the fluorescence intensity and the length of the 5′ overhang of the captured $bla_{SHV}$ and *tuf* product strand.** (A) Results for the $bla_{SHV}$ probe A-S-Shv1H691 hybridized to different $bla_{SHV}$ products of 183 to 715 bp. (B) Results for *tuf* probes hybridized to different area of the 523-bp *tuf* product amplified from *Staphylococcus hominis*. Probes A-S-TShoH520 (complementary to the lower strand) and A-S-TShoH520a (complementary to the upper strand) target the same region of the *S. hominis* product. For all panels, each value is the mean of three replicates. Standard deviation for these replicates is also shown.

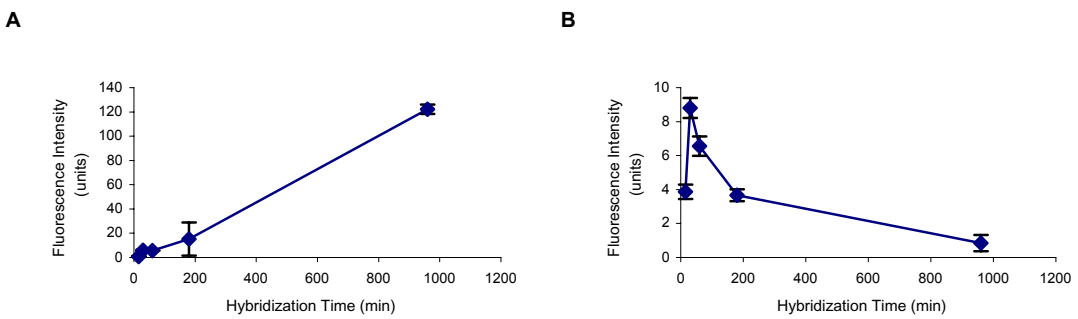


**Figure 4. Typical hybridization kinetics for captured product strands having different lengths of 5′ overhang.** (A) Example of a captured *ermB* product having a short 5′ overhang (A-S-ErmBH459; 62-bp overhang). (B) Example of a captured *ermB* product having a long 5′ overhang (A-S-ErmBH370; 261-bp overhang). For all panels, each value is the mean of three replicates. Standard deviation for these replicates is also shown.

ducible hybridization signals, while probes targeting the 3′ extremity of the captured target strand gave no or very weak hybridization signals after overnight hybridization. One plausible explanation is that T* hybridized by its 3′ end is less stable than the same strand hybridized closer to its 5′ end. To verify this hypothesis, hybridization kinetics were assessed by hybridizing the 432-bp labeled products with the *ermB* array for 15, 30, 60, and 180 min and 16 h. Probes targeting regions close to the 5′ end of either strand of the product showed a fluorescent signal increasing with hybridization time (Figure 4A). Probes targeting regions leaving a longer 5′ overhang of either strand of the products exhibited very different hybridization kinetics (Figure 4B). Indeed, we observed an increase of the hybridization signal in the first 30 min of hybridization, but thereafter fluorescence intensity decreased over time until it reached background levels.

To test the ability of the nonhybridized complementary strand (T′) to destabilize the T*P duplex, we carried out experiments with single-stranded products. Microarrays were hybridized for 10 h with the amplified 432-bp *ermB* product lower strand (T*) generated by asymmetrical PCR. After washing out the nonhybridized T* still in solution ($T^*_{free}$), the hybridization was carried out for an additional 16 h, either with hybridization buffer alone or with an equimolar amount of the complementary upper strand T′. In the presence of only single-stranded target DNAs (T*), the region at which the oligonucleotide probe hybridizes no longer influences the hybridization intensity. For example, probe A-S-ErmBH272, with a 5′ overhang of 249 nucleotides, hardly captures any of the target DNA when the double-stranded product is used as target (Figure 2A). However, this same probe efficiently captured the complementary single-stranded DNA produced by asymmetrical PCR (Figure 5A). Similar results were observed for hybridization with the upper product strand. The intensity of fluorescence decreased dramatically when the complementary T′ bottom strand was included in the assay (Figure 5B). The addition of the complementary strand T′ reduced the intensity of hybridization close to background levels, suggesting that T*P duplex destabilization occurs in the presence of the complementary strand.

## DISCUSSION

This work was initiated to study new parameters that could govern the hybridization efficiency of oligonucleotide capture probes arrayed onto a solid support. As described above, we observed that the position a capture probe targets on a given product has an impact on the observed hybridization signal. The sequence of the probe does not seem to modify this impact, and this phenomenon was observed on three different probe-product sets.

Interestingly, the hybridization behavior of a double-stranded product DNA on short oligonucleotides immobilized by their 5′ end gave counter-intuitive results. Indeed, one would assume weaker hybridization signal when a 5′ end immobilized probe binds the target molecule close to its 5′ end, because of steric hindrance caused by a longer 3′ overhanging tail. However, our results show that the increase of the 3′ end has no major effect on hybridization signal, whereas the hybridization signal strength is inversely correlated with the length of the 5′ overhanging tail of the target molecule when hybridized with a probe immobilized via its 5′ end.

This hybridization behavior could be explained by the topology of the T*P duplex. When a probe recognizes an area closer to the 3′ end of the captured target strand T*, most of the overhanging 5′ end of nonhybridized DNA is exposed to the liquid phase above the glass surface (Figure 6). On the other hand, when it hybridizes to an area close to the 5′ end of the captured strand target, most of T* (3′ end) is directed towards the glass surface. In the first conformation, the protruding tail of T* could be available for reassociation with its complementary strand (T′), a process that could destabilize the probe-target duplex (T*P) as shown when asymmetrical products were used. This hybridization behavior may also be observed with 3′ immobilized probes. However, experiments using 3′

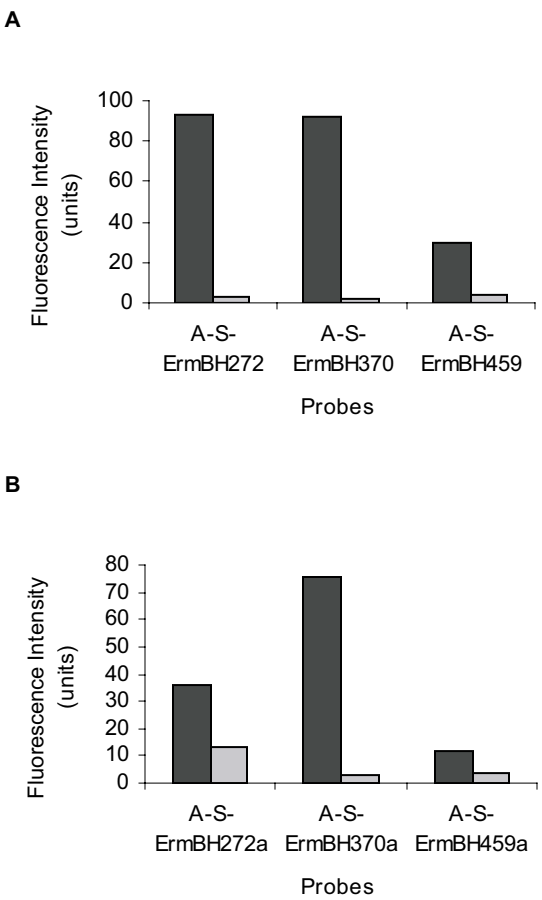


**Figure 5. Hybridization to a microarray of asymmetrical PCR-generated single-stranded target product strand (T*) followed by hybridization with the complementary product strand (T′).** T* was hybridized for 10 h to the *ermB* array. Nonhybridized T* ($T^*_{free}$) was then washed away, and the array was hybridized another 16 h with an equimolar quantity of the complementary strand T′ (grey boxes) or with hybridization buffer alone (black boxes). Slides were washed prior to fluorescence detection. A significant decrease in signal was observed when the complementary strand T′ was hybridized for 16 h compared to the control hybridization using buffer only. (A) Hybridization to the lower strand of the 432-bp product followed by hybridization with the upper strand of the product. (B) Hybridization to the upper strand of the 432-bp product followed by hybridization to the lower strand of the same product. For both panels, each result is the mean of three replicates.

immobilized capture probes have not been performed because such probes are rarely used.

Displacement of T* from P by reassociation with T′ could proceed through a sequential displacement pathway also known as a zipper effect (31). Hybridization between the captured T* strand and its complementary strand T′ in solution would occur first at the exposed overhang tail of captured T* and would be followed by a branch migration mechanism. Such a mechanism was used recently to build a DNA-fueled nanomolecular machine (32,33). In those studies, the authors used the complementary DNA strand (called fuel DNA) to close and open double-stranded DNA structures. We propose that the complementary strand T′ acts as the fuel DNA, thereby pulling the captured target strand T* from the probe (Figure 6).

By using asymmetrical PCR, we have shown that the captured product strand is displaced by the target complementary strand T′ independently of the area the probe targets on the product (Figure 5). This suggests that some elements stabilize T*P when the hybridizations were performed in the presence of both T* and T′. One possible model would be that $T^*_{free}$ forms a quaternary complex ($T^*T'T^*_{free}P$) with the ternary complex (T′T*P) captured on the glass surface. In accordance with the random walk theory for branch migration (34), the branch point between T*T′ and $T'T^*_{free}$ duplexes of the $T^*T'T^*_{free}P$ complex can move in either direction. The random walk would continue until one of two helices becomes shorter than the minimum length of a stable duplex (31). This means that the longer the duplex part of the helix is, the more likely it is to displace the other competing duplex (e.g., if T*T′ forms a longer helix, it would destabilize the complex $T'T_{free}$ and vice-versa).

Clearly, other parameters such as the secondary structure of probes and products may play a role in hybridization efficiency. For example, the efficiency of hybridization to capture probe A-S-ErmBH459 is not entirely explained by the model illustrated in Figure 6, since this probe, which targets a region close to the 5′ end of the product, gives a low hybridization signal.

In conclusion, we have clearly demonstrated a correlation between the region of the product targeted by a capture probe and the efficiency of hybridization using three different target genes as models. We have provided evidence that the presence of the complementary strand is associated with the poor hybridization efficiency of 5′ immobilized probes targeting the 3′ end of a product, thereby leaving a long 5′ overhang. On the other hand, probes targeting the 5′ end of the same product hybridized more efficiently. These results should contribute to the establishment of novel guidelines for the efficient design of capture probes, which should help to improve the sensitivity and specificity of microarray detection. This study demonstrates the importance of choosing the appropriate nucleic acid region to ensure efficient and sensitive detection of double-stranded DNA fragments such as PCR products using short capture probes. This is particularly important for SNP detection. In addition, efforts are ongoing to develop novel amplification and labeling systems for efficient production of single-stranded DNA products that would circumvent the competition between complementary strands.

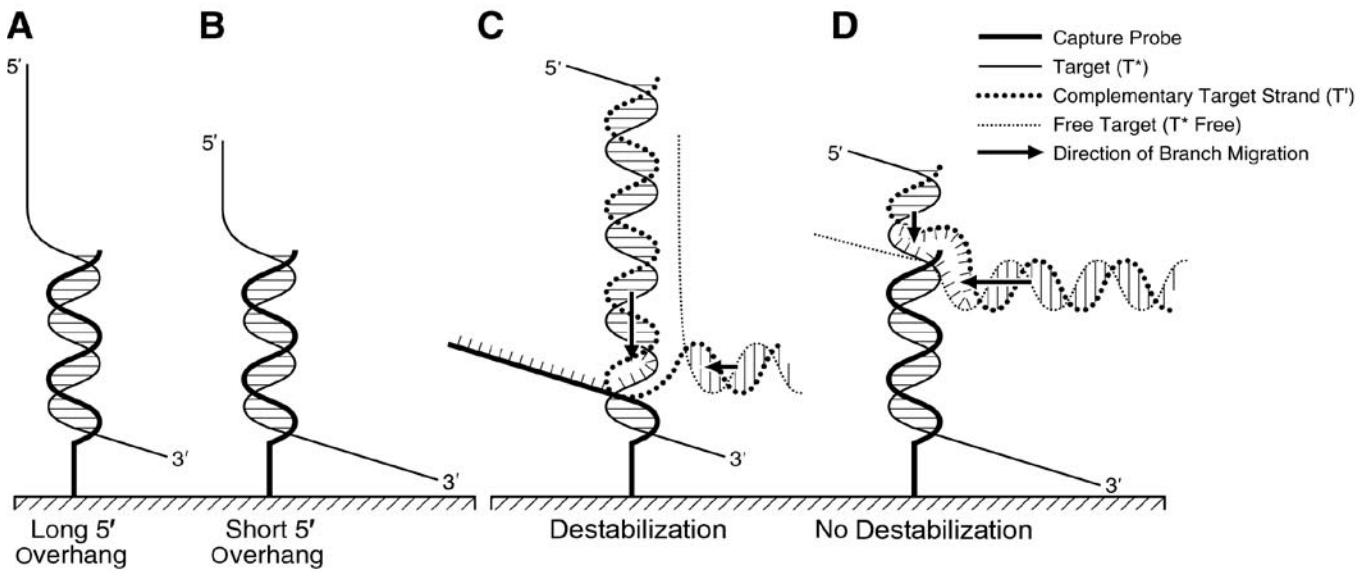


**Figure 6. Idealized interactions between an immobilized DNA probe and the two strands of the target product.** (A) The target strand (T*) hybridized to the DNA probe, leaving a long 5′ overhang of the captured product strand targeted by the probe. (B) The target strand (T*) hybridized to the DNA probe, leaving a short 5′ overhang of the captured product strand targeted by the probe. (C) The free complementary strand of the target product (T′) hybridized to the overhanging tail of T*, generating a branch migration that caused destabilization of the secondary complex. (D) The free T* ($T^*_{free}$) hybridized to the free region of T′, generating an antagonistic branch migration that prevented the first branch migration from breaking the secondary complex.

**ACKNOWLEDGMENTS**

*This research project was supported by Valorisation-Recherche Québec and Génome Québec/Genome Canada. M.O. is a Burroughs Wellcome Fund scholar in molecular parasitology and the holder of a Canada Research Chair in Antimicrobial Resistance.*

**COMPETING INTERESTS STATEMENT**

*The authors declare no competing interests.*

**REFERENCES**

1. **Debouck, C. and P.N. Goodfellow.** 1999. DNA microarrays in drug discovery and development. Nat. Genet. *21*:48-50.
2. **Duggan, D.J., M. Bittner, Y. Chen, P. Meltzer, and J.M. Trent.** 1999. Expression profiling using cDNA microarrays. Nat. Genet. *21*:10-14.
3. **Marton, M.J., J.L. DeRisi, H.A. Bennett, V.R. Iyer, M.R. Meyer, C.J. Roberts, R. Stoughton, J. Burchard, et al.** 1998. Drug target validation and identification of secondary drug target effects using DNA microarrays. Nat. Med. *4*:1293-1301.
4. **Cardoso, F.** 2003. Microarray technology and its effect on breast cancer (re)classification and prediction of outcome. Breast Cancer Res. *5*:303-304.
5. **Cromer, A., A. Carles, R. Millon, G. Ganguli, F. Chalmel, F. Lemaire, J. Young, D. Dembele, et al.** 2004. Identification of genes associated with tumorigenesis and metastatic potential of hypopharyngeal cancer by microarray analysis. Oncogene *23*:2484-2498.
6. **Ringner, M. and C. Peterson.** 2003. Microarray-based cancer diagnosis with artificial neural networks. BioTechniques *34*:S30-S35.
7. **Verpoorte, E.** 2002. Microfluidic chips for clinical and forensic analysis. Electrophoresis *23*:677-712.
8. **Davies, T.A. and R. Goldschmidt.** 2002. Screening of large numbers of *Streptococcus pneumoniae* isolates for mutations associated with fluoroquinolone resistance using an oligonucleotide probe assay. FEMS Microbiol. Lett. *217*:219-224.
9. **Mikhailovich, V., S. Lapa, D. Gryadunov, A. Sobolev, B. Strizhkov, N. Chernyh, O. Skotnikova, O. Irtuganova, et al.** 2001. Identification of rifampin-resistant *Mycobacterium tuberculosis* strains by hybridization, PCR, and ligase detection reaction on oligonucleotide microchips. J. Clin. Microbiol. *39*:2531-2540.
10. **Stenger, D.A., J.D. Andreadis, G.J. Vora, and J.J. Pancrazio.** 2002. Potential applications of DNA microarrays in biodefense-related diagnostics. Curr. Opin. Biotechnol. *13*:208-212.
11. **Kane, M.D., T.A. Jatkoe, C.R. Stumpf, J. Lu, J.D. Thomas, and S.J. Madore.** 2000. Assessment of the sensitivity and specificity of oligonucleotide (50-mer) microarrays. Nucleic Acids Res. *28*:4552-4557.
12. **Wang, R.F., M.L. Beggs, L.H. Robertson, and C.E. Cerniglia.** 2002. Design and evaluation of oligonucleotide-microarray method for the detection of human intestinal bacteria in fecal samples. FEMS Microbiol. Lett. *213*:175-182.
13. **Urakawa, H., S. El Fantroussi, H. Smidt, J.C. Smoot, E.H. Tribou, J.J. Kelly, P.A. Noble, and D.A. Stahl.** 2003. Optimization of single-base-pair mismatch discrimination in oligonucleotide microarrays. Appl. Environ. Microbiol. *69*:2848-2856.
14. **Guo, Z., R.A. Guilfoyle, A.J. Thiel, R. Wang, and L.M. Smith.** 1994. Direct fluorescence analysis of genetic polymorphisms by hybridization with oligonucleotide arrays on glass supports. Nucleic Acids Res. *22*:5456-5465.
15. **Chizhikov, V., A. Rasooly, K. Chumakov, and D.D. Levy.** 2001. Microarray analysis of microbial virulence factors. Appl. Environ. Microbiol. *67*:3258-3263.
16. **Peplies, J., F.O. Glockner, and R. Amann.** 2003. Optimization strategies for DNA microarray-based detection of bacteria with 16S rRNA-targeting oligonucleotide probes. Appl. Environ. Microbiol. *69*:1397-1407.
17. **Matveeva, O.V., S.A. Shabalina, V.A. Nemtsov, A.D. Tsodikov, R.F. Gesteland, and J.F. Atkins.** 2003. Thermodynamic calculations and statistical correlations for oligoprobes design. Nucleic Acids Res. *31*:4211-4217.
18. **Gao, H.F., S.C. Tao, D. Wang, C. Zhang, X. Ma, J. Cheng, and Y. Zhou.** 2003. Comparison of different methods for preparing single stranded DNA for oligonucleotide microarray. Anal. Lett. *33*:2849-2863.
19. **Tao, S.C., H.F. Gao, F. Cao, X.M. Ma, and J. Cheng.** 2003. Blocking oligo—a novel approach for improving chip-based DNA hybridization efficiency. Mol. Cell. Probes *17*:197-202.
20. **Reyes-Lopez, M.A., A. Mendez-Tenorio, R. Maldonado-Rodriguez, M.J. Doktycz, J.T. Fleming, and K.L. Beattie.** 2003. Fingerprinting of prokaryotic 16S rRNA genes using oligodeoxyribonucleotide microarrays and virtual hybridization. Nucleic Acids Res. *31*:779-789.
21. **Southern, E.M., S.C. Case-Green, J.K. Elder, M. Johnson, K.U. Mir, L. Wang, and J.C. Williams.** 1994. Arrays of complementary oligonucleotides for analysing the hybridisation behaviour of nucleic acids. Nucleic Acids Res. *22*:1368-1373.
22. **Antipova, A.A., P. Tamayo, and T.R. Golub.** 2002. A strategy for oligonucleotide microarray probe reduction. Genome Biol. *3*:research0073.1-research0073.4.
23. **Lockhart, D.J., H. Dong, M.C. Byrne, M.T. Follettie, M.V. Gallo, M.S. Chee, M. Mittmann, C. Wang, et al.** 1996. Expression monitoring by hybridization to high-density oligonucleotide arrays. Nat. Biotechnol. *14*:1675-1680.
24. **Lane, D.R., M.J. Krug, S.F. Gonzalez, and A. Warsen**. 2003. Amplicon secondary structure interferes with microarray hybridization. 103rd General Meeting of the American Society for Microbiology. Washington, DC.
25. **Shi, S.J., A. Scheffer, E. Bjeldanes, M.A. Reynolds, and L.J. Arnold.** 2001. DNA exhibits multi-stranded binding recognition on glass microarrays. Nucleic Acids Res. *29*:4251-4256.
26. **Steel, A.B., R.L. Levicky, T.M. Herne, and M.J. Tarlov.** 2000. Immobilization of nucleic acids at solid surfaces: effect of oligonucleotide length on layer assembly. Biophys. J. *79*:975-981.
27. **Roberts, M.C., J. Sutcliffe, P. Courvalin, L.B. Jensen, J. Rood, and H. Seppala.** 1999. Nomenclature for macrolide and macrolide-lincosamide-streptogramin B resistance determinants. Antimicrob. Agents Chemother. *43*:2823-2830.
28. **Rafalski, J.A.** 1988. Two strands of DNA are not equivalent as probes in hybridizations at low stringency. Anal. Biochem. *173*:383-386.
29. **Martineau, F., F.J. Picard, D. Ke, S. Paradis, P.H. Roy, M. Ouellette, and M.G. Bergeron.** 2001. Development of a PCR assay for identification of staphylococci at genus and species levels. J. Clin. Microbiol. *39*:2541-2547.
30. **Bradford, P.A.** 1999. Automated thermal cycling is superior to traditional methods for nucleotide sequencing of bla(SHV) genes. Antimicrob. Agents Chemother. *43*:2960-2963.
31. **Reynaldo, L.P., A.V. Vologodskii, B.P. Neri, and V.I. Lyamichev.** 2000. The kinetics of oligonucleotide replacements. J. Mol. Biol. *297*:511-520.
32. **Yurke, B., A.J. Turberfield, A.P. Mills, Jr., F.C. Simmel, and J.L. Neumann.** 2000. A DNA-fuelled molecular machine made of DNA. Nature *406*:605-608.
33. **Alberti, P. and J.L. Mergny.** 2003. DNA duplex-quadruplex exchange as the basis for a nanomolecular machine. Proc. Natl. Acad. Sci. USA *100*:1569-1573.
34. **Lee, C.S., R.W. Davis, and N. Davidson.** 1970. A physical study by electron microscopy of the terminally reptitious, circularly permuted DNA from the coliphage particles of *Escherichia coli* 15. J. Mol. Biol. *48*:1-22.

Received 18 January 2005; accepted 16 February 2005.

**Address correspondence to:**

Dr. Michel G. Bergeron
*Centre de Recherche en Infectiologie de l'Université Laval*
*Centre Hospitalier Universitaire de Québec*
*Pavillon CHUL*
*2705 Boul. Laurier*
*Sainte-Foy, Québec G1V 4G2, Canada*
*e-mail: Michel.G.Bergeron@crchul.ulaval.ca*